İSTANBUL UNIVERSITY
CERRAHPAŞA

ORIGINAL ARTICLE
Electrica 2022; 22(2): 287-294

Parameter Calculation and Structural Electric Field Optimization of Stress Cone for Main Insulation Layer of a 10 kV Cable

Jian Wu, Jing Xu, Weixun Qin, Jianfeng Wang, Mugen Wu

State Grid Zhejiang Electric Power Co., Ltd. Huzhou Power Supply Company Huzhou, Zhejiang, China

Cite this article as: J. Wu, J. Xu, W. Qin, J. Wang and M. Wu, "Parameter calculation and structural electric field optimization of stress cone for main insulation layer of a 10 kV cable," *Electrica.*, 22(2), 287-294, 2022.

ABSTRACT

In the entire power system operation, the cable is an essential and important component. However, the internal structure of the cable joint is complex and the material has diverse characteristics, which can easily lead to electric field distortion and power failure. Based on this, in order to reduce the occurrence of such problems and improve the safety of cable operation, this paper calculates and analyzes the stress cone parameters of the main insulation layer of a 10 kV cable, and optimizes its structural electric field. Specifically, the formulas of stress cone, reaction force cone, and thickness of the wound-insulating layer are designed, and the parameters are calculated. The results show that the maximum radius R_m of enhanced insulation is 28 mm, the thickness ΔR of enhanced insulation of the cable terminal is 13 mm, etc. The appropriate optimization parameters are then selected, and the electric fields of the shielded pipe structure, stress cone structure, and accessory body are optimized, and a reasonable optimization approach is given.

***Index Terms*—**Cable, electric field optimization, stress cone parameter

I. INTRODUCTION

At present, the unbalanced distribution of domestic power energy and load demand still exists, and it is necessary to use cables to realize the reasonable distribution of power energy. However, the loss caused by this transmission method is huge. If the state of the cable is not dynamically monitored, the electric field of the structure reasonably optimized, and the electric field uniformly distributed, problems such as insulation breakdown and cable intermediate joint defects will follow, which appear to inhibit the safe operation of the power system [1-4]. The optimization of the electric field of the cable structure needs to be based on the parameters of the stress cone. Therefore, when optimizing the electric field of the main insulation layer of the cable, the parameters of the stress cone need to be calculated and determined to provide a basis for the optimization of the cable structure [5-10]. Therefore, this paper will take the 10 kV cable as an example, starting with the calculation of stress cone parameters, and gradually analyze, complete the electric field optimization of the cable's main insulation layer structure, realize the reasonable control of electric field distribution, and ensure the safe and normal operation of the power system.

II. Design Principle of Structural Parameters of Stress Cone of Main Insulation Layer

Normally, the 10 kV cable's main insulation stress cone and its structural design method have three parameters. Firstly, the stress cone structure can be designed by using the electric field gradient vector modulus of each point on the cone curve. However, this method is restricted by model design and calculation, and therefore it is impossible to give an exact analytical formula. The optimal structure design scheme is usually obtained by electric field analysis. Although this mode cannot ensure that the electric field gradient at the junction of the stress cone and the added wound is smaller than the electric field gradient of the main insulation layer of the cable, its voltage tolerance value can reach the corresponding standard from beginning to end, that is, the voltage tolerance value of the added wound insulation is always greater than the electric field gradient modulus of the surface. Secondly, the design of the stress cone structure can be realized from the aspects of electric field gradient and interface pressure. This method not only takes into account the tangential electric field gradient at the interface, but also the correlation between the allowed tangential gradient of the stress cone and the interface pressure. Thirdly,

Corresponding author:
Jian Wu
E-mail: uw45q8@yeah.net

Received: October 9, 2021
Revised: November 12, 2021
Accepted: January 8, 2022
DOI: 10.54614/electrica.2022.210134

Content of this journal is licensed under a Creative Commons Attribution-NonCommercial 4.0 International License.

based on the consistency of the electric field gradient between the stress cone and the cable's main insulation layer, the design of the stress cone structure is completed. This is because the stress cone and the cable's main insulation layer are not only the important components of the cable terminal, but also the weak link. There are many scholars in China who use the third method to design and optimize the reaction force cone parameters of the cable's main insulation layer.

A. Design Formula of Stress Cone

The schematic diagram of stress cone design is shown in Fig. 1.

Let any point on the stress cone surface be represented by F(x,y). When the stress cone is connected to the shielding layer and the corresponding point is zero, the cable stress cone is an equipotential surface, that is, there is an orthogonal relationship between the power line of the terminal and the stress cone. In this case, the included angle between the radial direction and the power line at point F is represented by α. Thus, the relation between the tangential field strength E_t along the axis and the normal field strength E_n along the radial direction is shown in (1):

$$E_t = E_n \times \tan\alpha \tag{1}$$

The normal field strength E_n passing F can be calculated from (2):

$$E_n = \frac{U}{y\varepsilon_m\left(\frac{1}{\varepsilon_1}\ln\frac{R}{r_c}+\frac{1}{\varepsilon_m}\ln\frac{y}{R}\right)} = \frac{U}{y\left(\frac{\varepsilon_m}{\varepsilon_1}\ln\frac{R}{r_c}+\ln\frac{y}{R}\right)} \tag{2}$$

Through rearrangement, (3) can be obtained:

$$\int_0^x E_t dx = \int_R^y \frac{U}{y\left(\ln\frac{R}{r_c}\right)^{\frac{\varepsilon_m}{\varepsilon_1}}+\ln\frac{y}{R}}dy \tag{3}$$

Through the integral solution of (3), the conical structure design formula is obtained, as shown in (4):

$$x \approx \frac{U}{E_t}\ln\left(\frac{\ln\frac{y}{R}}{\ln\left[\left(\frac{R}{r_c}\right)^{\frac{\varepsilon_m}{\varepsilon_1}}\times\frac{y}{R}\right]}\right) \tag{4}$$

In the above equation, the axial coordinates are represented by x and the radial coordinates by y. The tangential electric field intensity on the stress cone surface is represented by E_t, and the normal electric field intensity is represented by E_n. The dielectric constant of insulation material is represented by ε_m, and the dielectric constant of cable body is represented by ε_1. The radius of the main insulation layer of the cable is represented by R, the voltage of the cable core to the ground and the radius of the conductor layer are represented by U and r_c, respectively. At this time, assuming $x=L$, $y=R_m$, the obtained stress cone length formula is shown in (5):

$$L = \frac{U}{E_t}\ln\left(\frac{\ln\frac{R_m}{R}}{\ln\left[\left(\frac{R}{r_c}\right)^{\frac{\varepsilon_m}{\varepsilon_1}}\times\frac{R_m}{R}\right]}\right) \tag{5}$$

In (5), the increased insulation thickness is represented by R_m.

B. Design Formula of Reactive Force Cone

In the 10 kV cable terminal joint, in order to reasonably control the axial field strength at the insulated end of the cable body, it is necessary to cut the insulated end into a conical surface opposite to the stress cone surface, that is, into a reaction force cone. Among them, the reactive force cone refers to the interface between the winding insulation at the cable terminal and the insulation of the cable body. In the cable connector, the interface is a key part and a weak link. If it is not handled well during the installation, the sliding breakdown problem is likely to occur [11]. The design formula of the reaction force cone is as follows:

$$x = \frac{U}{E_t}\times\frac{\ln\frac{y}{r_c}}{\ln\left[\left(\frac{R_m}{y}\right)^{\frac{\varepsilon_1}{\varepsilon_m}}\times\frac{R}{r_c}\right]} \tag{6}$$

In this case, assuming $x=L_c$, $y=R$, the obtained formula for the length of the reaction force cone is shown in (7).

$$L_c = \frac{U}{E_t}\times\frac{\ln\frac{R}{r_c}}{\ln\left[\left(\frac{R_m}{R}\right)^{\frac{\varepsilon_1}{\varepsilon_m}}\times\frac{R}{r_c}\right]} \tag{7}$$

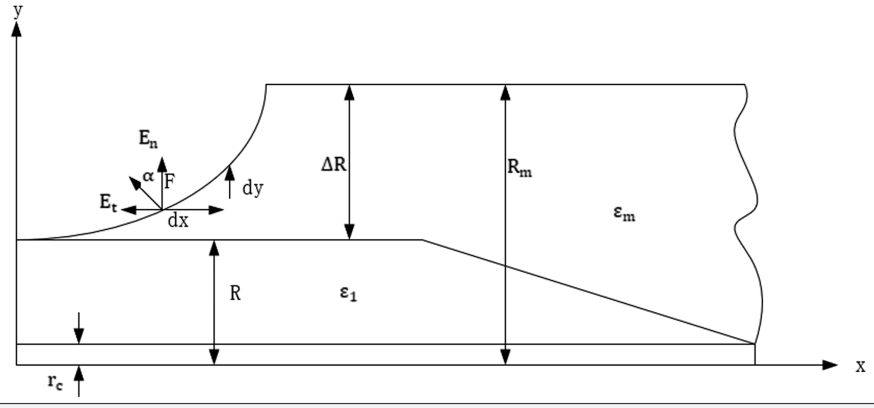

Fig. 1. Stress cone design diagram.

C. Design Formula of Winding Insulation Thickness

The determination of the winding insulation thickness involves the rated voltage grade of the cable and the voltage strength of the insulating material at the end of the cable. The specific design formula is shown in (8):

$$E_m = \frac{U}{r_c \ln \frac{R_m}{r_c}} \tag{8}$$

Expression 8 can be rearranged to obtain (9):

$$R_m = r_e exp\left(\frac{U}{r_c E_m}\right) \tag{9}$$

The formula for increasing the insulation thickness of the cable terminal is shown in (10):

$$\Delta R = R_m - R = r_c \exp\left(\frac{U}{r_c E_m}\right) - R \tag{10}$$

III. CALCULATION AND ANALYSIS OF THE STRUCTURAL PARAMETERS OF THE REACTIVE FORCE CONE OF THE MAIN INSULATION LAYER

A. Cable Stress Cone Material Selection

The insulation size will be different with different stress cone materials, so it is necessary to pay attention to the selection of stress cone materials. If the electrical strength of the selected material is insufficient, it needs to be adjusted by intervention measures such as increasing the thickness of the stress cone and the rubber protective sleeve insulation. However, under this intervention behavior, the electric field of the middle structure of the cable accessory is affected and thus changed. In addition, for stress cone semi-conductive insulating material, its uniform conductivity is also the key. If the performance of the stress cone semi-conductive insulating material is poor, then its electric field performance will be inhibited, causing insulation accidents. Today, ethylene propylene diene rubber (EPDM) and silicone rubber (SIR) are the first choice of stress cone materials, and the properties of both materials are shown in Table I.

In addition to the performance disclosed above, EPDM also has the advantages of high hardness, strong tear resistance, high breakdown strength of power frequency, high elastic modulus, and good compatibility with silicone oil, so it can be applied to the stress cone products with a mechanical compression device. The holding force of the cable–insulation interface can be improved by EPDM, which has good interface characteristics. Using EPDM to make the stress cone can give full play to its electrical breakdown performance, reduce its geometric size, and improve the electrical insulation margin. Silicone rubber, in addition to the performance shown in the table, also has good hydrophobicity, weather resistance, elastic elongation, and leakage trace resistance, and is usually used in the production of low and medium pressure cold-shrinkable homes, cold-shrinkable intermediate joints, indoor and outdoor terminals, and other products. As the research object of this paper is the 10 kV cold-shrinkable intermediate joint, SIR is selected as the material for making the stress cone.

TABLE II. STRUCTURAL PARAMETERS OF THE 10 KV CABLE

Sequence	Structure	Outer Diameter (mm)
1	A conductor layer	20.6
2	Insulating layer	31
3	The outer sheath layer	37.7
4	Insulating shield	32.6

B. Calculation of Stress Cone Parameters

It can be seen from the calculation formula of the 10 kV cable terminal stress cone that the length of the reactive force cone, the length of the stress cone, and the thickness of the wound insulation should be determined on the basis of the structural parameters of the 10 kV cable. Its structural parameters are shown in Table II.

The stress cone is an important part of cable accessories, which is responsible for controlling the electric field's uniform distribution of cable–insulation interface. By changing the shape and length of the stress cone, the maximum axial stress of the cable insulation surface can be ensured to be consistent with the maximum allowable axial stress of the cable's internal insulation, so that the distribution of the field strength near the metal cable sheath is uniform, and the electric field can be optimized. In order to calculate the length of the reaction force cone, the length of the stress cone, and the thickness of the winding insulation, relevant parameters need to be determined. Make the maximum rated voltage U of the 10 kV cable 12 kV, the value space of the axial electric field strength of the stress cone is 0.2–0.3 kV/mm, the dielectric constant ε_1 of the SIR is 2.8, and the dielectric constant ε_m of the insulation of the cable is 2.3. The main insulation radius R is 15.05 mm, and the conductor radius r_c is 8.05 mm. In the calculation process, the rated voltage U of the cable is set to 10 kV. Since the main insulation of the cable body can be regarded as a cylinder, the electric field distribution of the insulation body can be calculated by (11)[12].

$$E_x = \frac{U}{r_x \ln \frac{R}{r_c}} \tag{11}$$

In the formula, r_x is the distance from the electric field point to the center point.It can be seen from (11) that the electric field intensity

TABLE I. PROPERTIES OF TWO KINDS OF STRESS CONE MATERIALS

Material	Loss Coefficient	Dielectric Constant	Tensile Strength (MPa)	Volume Resistivity (Ω·cm)	Manufacturability
EPDM (≥35 kV/mm)	≤0.004	2.5–3.5	≥5	1017	Difficult
EPDM (≥300 kV/mm)	Moderate	0.86–0.87	Good	50–75	General
SIR (≥20 kV/mm)	≤0.004	2.8–3.5	≥5	2*1015	Easy
SIR (≥400 kV/mm)	Moderate	1.15–1.38	Good	30–50	Poor

TABLE III. THEORETICAL CALCULATION OF STRUCTURE OF A CABLE STRESS CONE

Increase the Winding Insulation Thickness	Length of Stress Cone	Reactive Force Cone Length
15 mm	25 mm	20 mm

will increase with the shortening of the distance between the electric field point and the outer layer, but this increase is not unlimited, and the maximum value will be generated at the interface between the conductor layer and the insulation layer. Combined with the parameters set above, the maximum allowable working field strength E_{max} of the cable is calculated as shown below.

$$E_{max} = \frac{U}{r_c \ln \frac{R}{r_c}} = \frac{10}{8.05 \ln \frac{15.05}{8.05}} = 1.98\ \text{kV / mm} \quad (12)$$

Similarly, insert the set parameters into (9), and it can be concluded that the maximum radius of enhanced insulation R_m is 28 mm; then calculate that the cable terminal insulation thickness ΔR is 13 mm by using (10), and the stress cone length L is 21.27 mm by using (5) (the transverse field strength E_t is 0.29). According to (7), the length of the reaction force cone L_c is 18.72 mm. Through the above calculation results, the calculation results of the 10 kV cable stress cone are summarized in Table III.

IV. OPTIMIZATION ANALYSIS OF STRUCTURAL ELECTRIC FIELD BASED ON STRESS CONE PARAMETERS

A. Optimization Parameter Selection

The uniform electric field can be obtained by controlling the electric field distribution of the internal interface of the cable joint by the stress cone, so as to optimize the concentration of the field intensity at the metal protective sleeve of the shielding layer and the edge of the point stress joint system. Therefore, the stress cone parameters mainly include the length of the stress cone and the radius of curvature of the end, and the structural electric field of the system can be optimized by setting these parameters. In addition, in order to overcome the influence of high potential at the cable junction, a Faraday cage will be formed at the main insulation of the cable. It can be seen that the shape and length of the shielded tube port should be reasonably controlled, so as to effectively optimize the structural electric field. When the shielding tube is too long, the accessory body will be too long; otherwise, it will limit the shielding effect of the shielding tube, resulting in the problem of high potential concentration at the junction. In addition, the distance between the stress cone and the shielded tube will also affect the length of the cable accessory body. When the distance between the stress cone and the shielded tube is not between the set values, the electric field distribution of the cable accessory body will be negatively affected. Therefore, it is also necessary to optimize the length of the cable accessory body.

B. Optimization of the Electric Field of Shielded Tube Structure by Stress Cone Parameters

The electric field of shielded tubes with different port shapes is optimized and simulated by using stress cone parameters. There are six different port shapes of shielded tubes, such as 0°, 30°, 45°, 60°, 90°, and 1/4 arc at the central angle of the end. The final results are shown in Fig. 2 and 3.

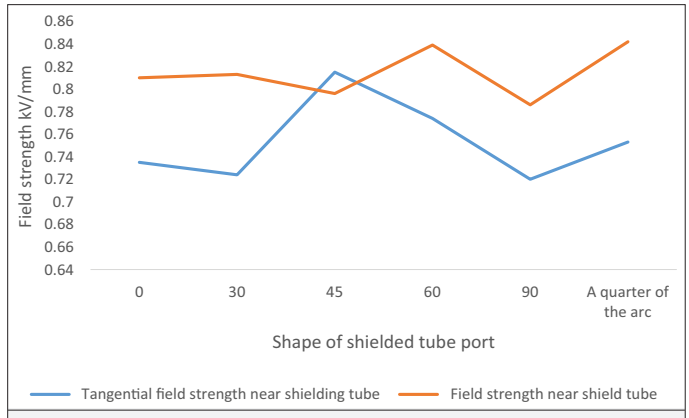

Fig. 2. Distribution of field strength and tangential field strength at the port of shielded tube.

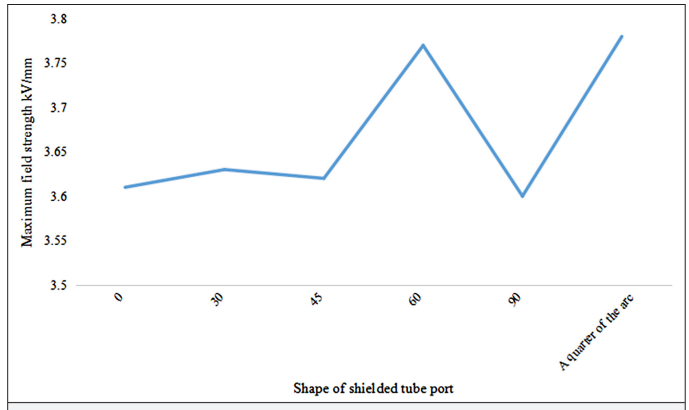

Fig. 3. Variation of maximum field strength of shielded tubes with different port shapes.

As can be seen from Fig. 2 and 3, when the shielded tube port is 90°, the field strength (tangential field strength, field strength at the shielded tube, and maximum field strength) is the smallest, which is the best choice for optimizing the structural electric field. At present, many cable accessory manufacturers will cut both ends of the shielded tube at 90° to form a right angle, but this is not useful for improving the field strength. Therefore, it is worth optimizing from the perspective of field strength optimization. After optimizing the structure of shielding tubes with different ends, it is necessary to design their length reasonably to optimize the electric field of the structure. Specifically, the electric field strength of seven shielded tubes with different lengths (130 mm, 135 mm, 140 mm, 145 mm, 150 mm, 155 mm, and 160 mm) is optimized and simulated, and the results are shown in Fig. 4 and 5.

It can be seen from Fig. 4 and 5 that shielded tubes with different lengths have no significant influence on field strength. Although the field strength of the shielded tube is relatively small at 130 mm and 160 mm, the tangential field strength of the shielded tube accessories is relatively large. In conclusion, the 150 mm shielded tube is the best choice. The interaction of six different port shapes and seven different lengths of shielded tubes of indirect connectors in cables is simulated and calculated, and the results are shown in Fig. 6.

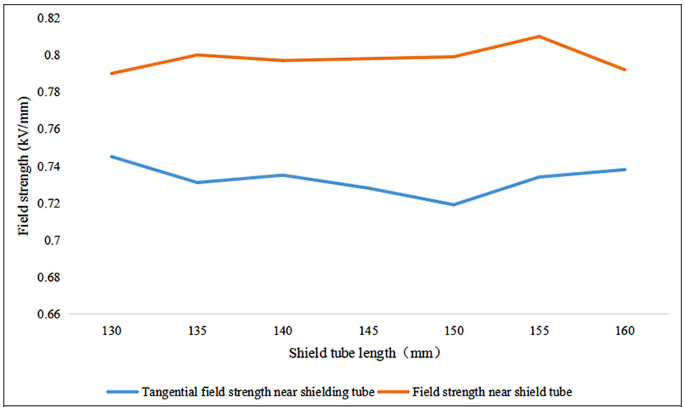

Fig. 4. Changes of field strength and tangential field strength at ports of shielded tubes with different lengths.

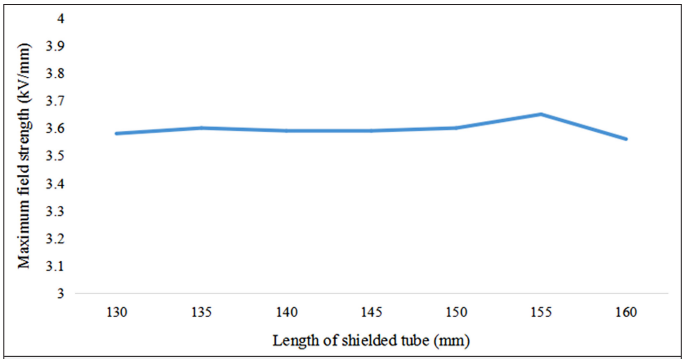

Fig. 5. Variation of maximum field strength of shielded tubes with different lengths.

In conclusion, the selection of 150 mm length of the shielded tube combined with a 90° port shielded tube can better optimize the structural electric field.

C. Optimization of Stress Cone Parameters on the Electric Field of Stress Cone Structure

Generally, the thickness of the stress cone of 10 kV cable accessories is basically kept at about 3 mm, so four kinds of stress cones of differing thickness (2 mm, 2.5 mm, 3 mm and 3.5 mm) are selected for optimization simulation calculation, and the results are shown in Fig. 7.

As can be seen from Fig. 6, stress cones of differing thickness have no significant influence on the field strength, so the stress cone thickness of 2.5 mm is selected to optimize the electric field of the structure. The structural electric field is then optimized by designing different stress cone lengths. Specifically, six stress cones (no stress cone, 25 mm, 35 mm, 45 mm, 55 mm, and 65 mm) with different lengths were designed for simulation analysis, and the results are shown in Fig. 8.

As can be seen from Fig. 8, the maximum field strength without stress cone is 5 kV/mm, and the tangential field strength is 3.55 kV/mm. After the length of the stress cone is changed, the maximum electric field strength of the axial component of the electric field is close to the average value of the electric field strength in the internal insulation

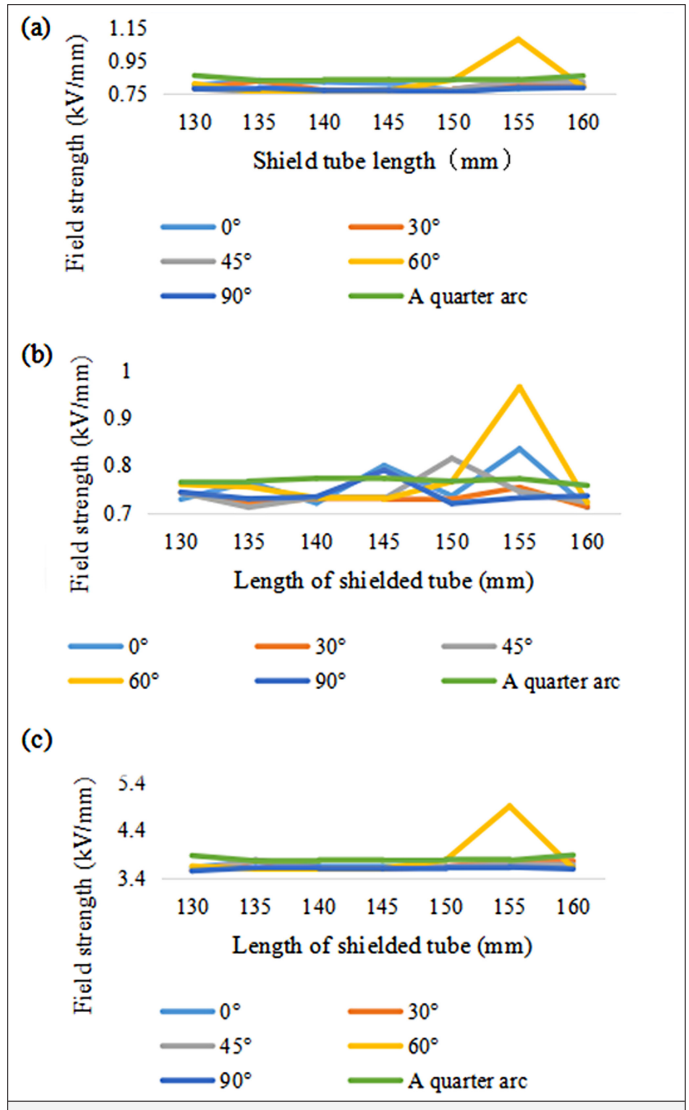

Fig. 6. The electric field changes under different lengths and shapes of shielded tubes.

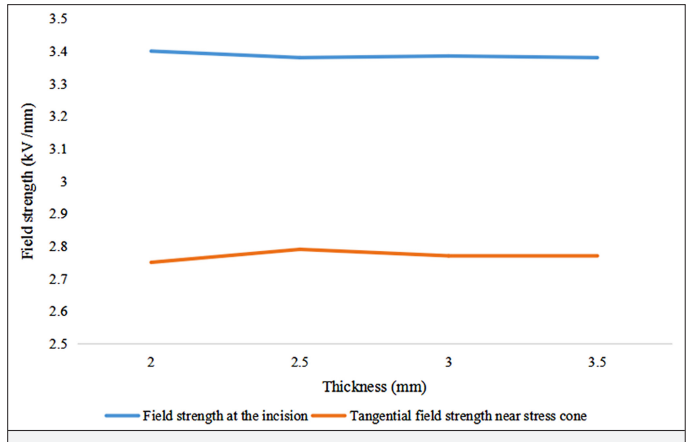

Fig. 7. Field strength variation of stress cones with different thickness.

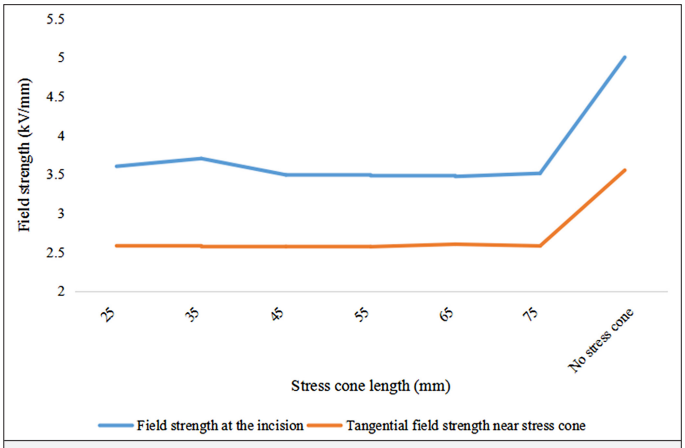

Fig. 8. Field strength variation of stress cones with different lengths.

of the cable. It can be seen that an excessively small length of stress cone will lead to the increase of field strength, as the two parameters are inversely proportional to each other. When the length is 45 mm, 55 mm and 65 mm, various performance indexes are concentrated. From the perspective of fabrication and installation, the stress cone of 55 mm length was selected to optimize the electric field of the structure. After selecting the length of the stress cone, reasonable consideration should be given to the curvature radius parameters of the stress cone end to realize the reasonable optimization of the structural electric field. Specifically, four stress cones with different curvature radii (15 mm, 20 mm, 25 mm, and 30 mm) are selected for simulation calculation, and the results are shown in Fig. 9.

As can be seen from Fig. 8, the field strength (notch field strength) decreases with the increase of curvature radius at the ends, and the two are inversely proportional. Although the uniform distribution of the electric field can be controlled by increasing the curvature radius of the stress cone, it should not be increased limitlessly. Therefore, it should be kept in check to avoid shortening the distance between the stress cone end and the insulation layer due to the excessive curvature radius, which will increase the field intensity on the surface of the insulation layer and adversely affect the anti-flashover performance of external insulation. Therefore, a 25 mm radius of curvature is suitable. In order to further analyze the influence of stress cone length and curvature radius of end on structural

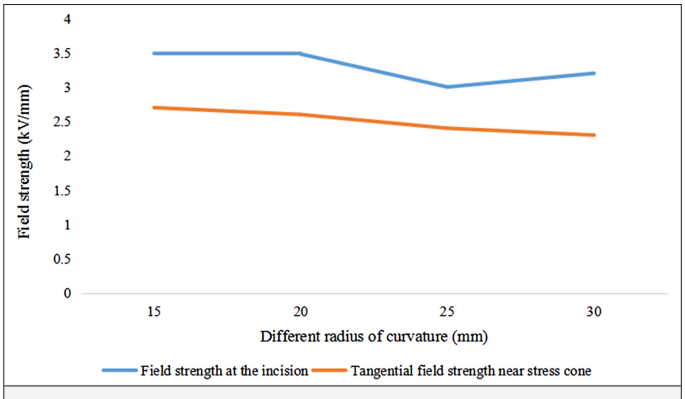

Fig. 9. Electric field variation of structure at stress cones with different end curvature radii.

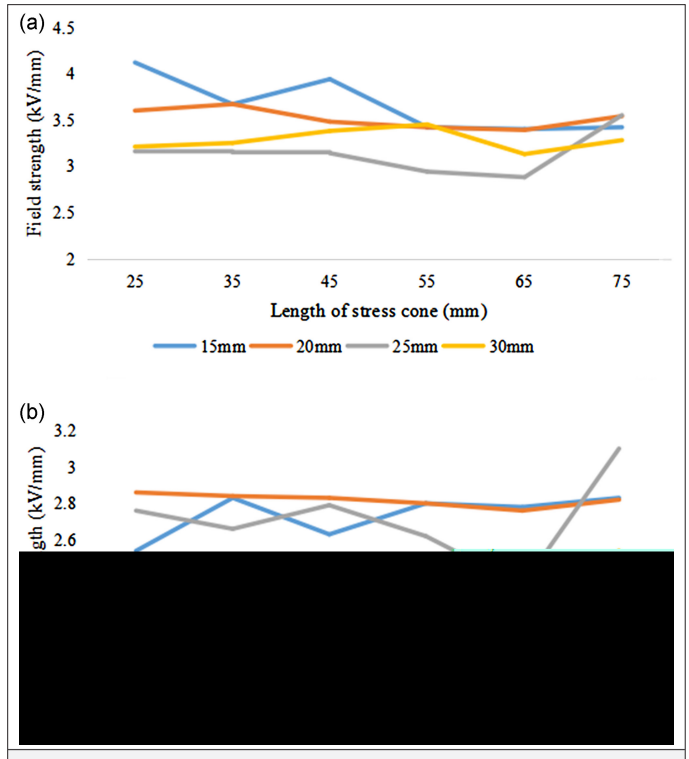

Fig. 10. The electric field changes under the pairing of different stress cone lengths and end curvature radii.

electric field, the interaction of stress cones with six different lengths and four different curvature radii of the ends of indirect joints in cables is simulated, and the results are shown in Fig. 10.

As can be seen from Fig. 10, a stress cone that is too large or too small is not conducive to the optimization of the electric field. When the radius of curvature is 25 mm, the maximum field strength is relatively low; when the radius of curvature is 30 mm, the tangential field strength of the stress cone is the smallest, but compared with the maximum field strength when the radius of curvature is 25 mm, the field strength of the stress cone is larger. Although increasing the curvature radius of the stress cone can reasonably control the distribution of electric field, too large a curvature radius will also have the opposite effect, resulting in the increase of electric field strength and interference with the flashover resistance of external insulation. At the same time, when the stress cone length is 55 mm and the radius of curvature is 25 mm, and when the stress cone length is 65 mm and the radius of curvature is 25 mm, both the maximum field strength and the tangential field strength of the stress cone are lower than the air breakdown field strength by 3 kV/mm. Therefore, it is reasonable to select 55 mm in length and 25 mm in curve radius of the cable insulation layer to optimize the structural electric field.

D. Electric Field Optimization of the Accessory Body

In order to analyze the length between the stress cone and the shielded tube, six different lengths of attachment body (30 mm, 40 mm, 50 mm, 60 mm, 70 mm, and 80 mm) were selected for simulation calculation and analysis, so as to screen out the most appropriate length between the stress cone and the shielded tube and realize the optimization of the electric field. The calculation results are shown in Fig. 11.

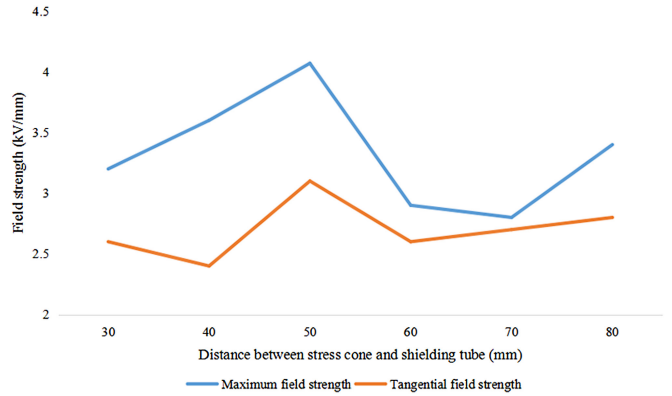

Fig. 11. Electric field variation between stress cones and shield tubes at different lengths.

As can be seen from Fig. 11, too large or too small a distance between the stress cone and the shielded tube is not conducive to the uniform distribution of the electric field of the accessory body. When the spacing is 30 mm and 40 mm, the maximum tangential field strength is the smallest, but it cannot meet the demand of less than the air breakdown field strength. When the spacing is 60 mm and 70 mm, both the maximum synthetic field strength and the tangential field strength meet the requirements of air breakdown field strength, that is, less than 3 kV/mm. This fixture can be selected to optimize the electric field distribution of the accessory body. However, as the spacing increases, the body length of the middle connector of the cable will increase, which is not conducive to the subsequent production. Therefore, the spacing of 60 mm is suitable.

V. CONCLUSION

In general, this paper first designs and proposes the calculation formula of the 10 kV cable stress cone, reaction force cone, and wound insulation thickness, which lays a foundation for the subsequent calculation of stress cone parameters. Secondly, based on the formula design, the cable stress cone parameters are calculated, including the maximum allowable working field strength of the cable, the maximum radius of enhanced insulation, the cable terminal insulation thickness, and the length of the stress cone. Finally, after fully determining the relevant parameters of the stress cone, the electric field of the shielded tube structure is simulated and optimized. The final conclusion is that the 150 mm length of the shielded tube combined with the 90° port of the shielded tube can better optimize the electric field of the structure. Then, the electric field of the stress cone structure is simulated and optimized. The final conclusion is that it is reasonable to select 55 mm and 25 mm curve radii to optimize the electric field of the structure. In the electric field simulation on optimization of the length of the accessory body, it is concluded that it is more appropriate to choose the distance between the stress cone and the shielded tube as 60 mm.

Peer-review: Externally peer-reviewed.

Author Contributions: Concept – J.W., J.X., W.Q.; Design – J.W., J.X., M.W.; Supervision – J.W, J.W., M.W.; Resources – J.W., J.X., J.W.; Data Collection and/or Processing – J.W., J.X., W.Q.; Analysis and/or Interpretation – J.W., J.X., M.W.; Literature Search – J.W., J.W., M.W.; Writing Manuscript – J.W., J.X., W.Q.

Declaration of Interests: The authors have no conflicts of interest to declare.

Funding: The authors declared that this study has received no financial support.

REFERENCES

1. L. Guo *et al.*, "Optimization research on improving the distribution of distortion electric field by nonlinear stress control tube of on-board cable terminal," *J. China Railw. Soc.*, vol. 43, no. 02, pp. 61–70, 2021.
2. J. Wu, Q. D. Shi, S. Li, and C. Y. Wen, "Influence of decentralized coordinated control of doubly-fed units with cable selection on reactive power optimization of wind power plant," *J. Electr. Power Sci. Technol.*, vol. 35, no. 02, pp. 113–119, 2020.
3. Z. X. Chen *et al.*, "Chen GZ. Research on electric field distribution and structural optimization of integrated prefabricated and wrapped XLPE HVDC cable joints," *J. Harbin Univ. Sci. Technol.*, vol. 23, no. 06, pp. 77–81, 2018.
4. Z. P. Jiang, J. Y. Song, and W. Yao, "Application of finite element combined with particle swarm optimization and differential evolution algorithm to electric field optimization of cable," *J. Electr. Power*, vol. 31, no. 01, pp. 47–52+83, 2016.
5. H. C. Xie, S. Hu, F. X. Huang, and H. Z. Huang, "Typical Fault Case analysis of cable terminal of 10kV ring network cabinet," *Mechan. Electr. Inform.*, no. 12, pp. 14–16, 2021.
6. H. Wang, and A. Q. Ma, "Simulation and improvement measures of air gap defect of prefabricated stress cone in high temperature superconducting cable terminal," *Hydropower Energ. Sci.*, vol. 37, no. 08, pp. 180–182, 2019.
7. Z. E. Zhu *et al.*, "Design of stress cone for flexible dc cable accessories," *Insul. Mater.*, vol. 52, no. 06, pp. 86–91, 2019.
8. T. Xu, C. Jia, and S. Xu, "Research on the size of stress cone for high voltage power accessories -- Taking 500 kV cable as an example," *Commun. Power Technol.*, vol. 35, no. 06, pp. 41–43, 2018.
9. X. J. Zhou, "Optimization design of multi-interface stress cone for high voltage cable terminal," *Bull. Sci. Technol.*, vol. 34, no. 05, pp. 180–183, 2018.
10. W. Wang, D. X. He, P. X. Song, X. R. Wang, F. S. Meng, and Q. Q. Li, "Effect of combined electrothermal aging on space charge accumulation characteristics at stress cone of cable accessories," *High Voltage Technol.*, vol. 45, no. 06, pp. 1737–1744, 2019.
11. J. Y. Zhuo, *Design Principle of Power Cable*. Beijing: China Machine Press, 1999.
12. Y. Xin, *Conducting Power Cables of Superconductors*. Beijing: China Electric Power Press, 2013.

Jian Wu, born in 1973, has received the bachelor's degree from Shanghai University of Electric Power in 2011. He is a senor engineer. He is interested in enterprise management, engineering construction management, power grid operation and maintenance management.

Jin Xu, born in 1974, has received the bachelor's degree from Shanghai University Of Electric Power in 2003. He is a senior engineer. He is interested in enterprise management, engineering construction management, power grid operation and maintenance management.

Weixun Qin, born in 1978, has received the master's degree from Donghua University. He is a senior engineer. He is interested in enterprise management, engineering construction management, power grid operation and maintenance management.

Jianfeng Wang, born in 1980, has received the master's degree from Zhejiang University in 2003. He is an engineer. He is interested in enterprise management, engineering construction management, power grid operation and maintenance management.

Mugen Wu, born in 1977, born in 1977, has received the bachelor's degree from Shanghai University of Electric Power in 2013. He is a senior engineer. He is interested in enterprise management, engineering construction management, power grid operation and maintenance management.